第 30 卷第 5 期
2014 年 5 月

无 机 化 学 学 报
CHINESE JOURNAL OF INORGANIC CHEMISTRY

Vol.30 No.5
1143-1150

具有类白钨矿结构的 $KGd(MoO_4)_2$ 的晶体结构和能带结构

赵 丹*,[1] 赵恩晓[1] 辛 霞[2] 李飞飞[1]

([1]河南理工大学物理化学学院,焦作 454000)

([2]山东大学国家胶体材料工程技术研究中心,济南 250100)

摘要: 以 Gd_2O_3、K_2CO_3、MoO_3 为原料,采用高温熔盐法,合成了一个含钾的稀土钼酸盐 $KGd(MoO_4)_2$。通过 X 射线单晶衍射法测定了它在室温下的晶体结构,并测定了它的光学性质。结构分析表明它属于三斜晶系,空间群为 $P\bar{1}$,a=0.529 23 (6) nm,b=0.692 10(6) nm,c=1.068 89(7) nm,α=75.79(8)°,β=76.79(5)°,γ=67.60(4)°,Z=2,R_1(all data)=0.025 8。结构中的 K 和 Gd 原子位于各自的晶体学位置,不存在调制结构的现象。此外,我们用得到的晶体学数据,通过密度泛函理论研究了化合物的能带结构、态密度、介电常数,其结果和实验数据相吻合。

关键词: 晶体结构; 稀土钼酸盐; 能带结构

中图分类号: O766+4; O741+3 **文献标识码**: A **文章编号**: 1001-4861(2014)05-1143-08

DOI: 10.11862/CJIC.2014.101

Single-Crystal Structure and Bond Structure of Scheelite-Like $KGd(MoO_4)_2$

ZHAO Dan*,[1] ZHAO En-Xiao[1] XIN Xia[2] LI Fei-Fei[1]

([1]*Department of Physics and Chemistry, Henan Polytechnic University, Jiaozuo, Henan* 454000, *China*)

([2]*National Engineering Technology Research Center For Colloidal Materials, Shandong University, Jinan* 250100, *China*)

Abstract: High-temperature reaction of Gd_2O_3, K_2CO_3 and MoO_3 leads to a potassium lanthanide molybdate, namely, $KGd(MoO_4)_2$. The structure of $KGd(MoO_4)_2$ was investigated by means of single-crystal X-ray diffraction at room temperature. Structural analysis results show that it crystallizes in triclinic space group $P\bar{1}$ with a=0.529 23(6) nm, b=0.692 10(6) nm, c=1.068 89(7) nm, α=75.79(8)°, β=76.79(5)°, γ=67.60(4)°, Z=2 and R_1(all data)=0.025 8. K and Gd atoms occupy their respective crystallographic distinct sites. No occupancy disorder and structural modulation exist in the structure. Furthermore, the obtained crystallographic data are used to calculate the band structure, density of states and dielectric constants with the density functional theory method. The results tend to support the experimental data. CSD: 427391.

Key words: crystal structure; lanthanide molybdate; bond structure

0 Introduction

Interest in the synthesis and characterization of rare-earth double molybdate crystals with general formula $ALn(MO_4)_2$ (A=alkali metal; Ln=rare-earth elements; M=Mo,W) arises mainly from the intriguing potential properties (magnetism, electricity, optics), as well as a wide variety of potential applications of the materials[1]. They are attractive solid-state laser host materials for their large rare-earth ion admittance. Most of these crystals have a tetragonal symmetry with the scheelite-type ($CaWO_4$)[2] structure (space group

收稿日期:2013-06-07。收修改稿日期:2013-11-08。

国家自然科学基金(No.21201056)和河南省科技厅(No.122300410418)资助项目。

*通讯联系人。E-mail: iamzd@hpu.edu.cn

$I4_1/a$) at room temperature, which can be thought of as the substitution of two Ca^{2+} ions in the $CaWO_4$ by a couple of M^+ and Ln^{3+} ions in either an ordered or a statistical manner. The differences of the radius of the considered M^+ and Ln^{3+} ions give rise to several structural families, such as $LiLa(MoO_4)_2$[3] (space group $Pbca$), $LiCe(MoO_4)_2$[4] (space group $P2_1/c$), $RbPr(MoO_4)_2$[5] (space group $Pnnn2$), $CsPr(MoO_4)_2$[6] (space group $Pccm$), α-$KEu(MoO_4)_2$[7] (space group $P\bar{1}$), $KY(MoO_4)_2$[8] (space group $Pbcn$), and $CsDy(MoO_4)_2$[9] (space group $P2/c$), etc. Especially, compounds $KLn(MoO_4)_2$ (Ln=La, Nd, Sm, Eu)[10] feature (3+1)-dimensional incommensurate modulated structure with super space group $I2/b(\alpha\beta0)00$ SSG and lattice constants $a \approx b \approx 0.55+0.05$ nm, $c \approx 2a$, $\gamma \approx 90°$. Their structural modulation may arise from the ordering of K/Ln atoms within the structure.

An examination of literature shows that previous structural studies on the compound $KGd(MoO_4)_2$ are confined to X-ray powder diffraction (XRD)[11], and the analysis of the structural characterization in detail through X-ray crystal structural determination has not been done. So we are making efforts to grow single crystals in the system and determine the crystal structure by single-crystal X-ray diffraction analysis, which are very meaningful for further studies on this extensive family of compounds. In this paper, we present synthesis, crystal structure of rare-earth double molybdate $KGd(MoO_4)_2$ at room temperature. At the same time, we make the calculations of crystal energy band structures and optical response function to explore the chemical bonding properties and electronic origin of optical transition of the title compound.

1 Experimental

1.1 Synthesis

Single crystals of $KGd(MoO_4)_2$ were prepared by the high temperature solution reaction, using analytical reagents of Gd_2O_3, K_2CO_3 and MoO_3 at the molar ratio of $n_{Gd}:n_K:n_{Mo}=1:1:2$. Starting mixture was finely ground in an agate mortar to ensure the best homogeneity and reactivity, and transferred to a platinum crucible to heat at a temperature of 773 K for 8 h. The obtained product was reground and heated at 1 173 K for 20 h, and then cooled to 973 K at a rate of 4 $K \cdot h^{-1}$. After heating at 973 K for 20 h, the mixture was cooled to 873 K at a rate of 2 $K \cdot h^{-1}$ and finally quenched to room temperature. In order to confirm the chemical composition of the compound, microprobe elemental analysis was performed on a field emission scanning electron microscope (FESEM, JSM6700F) equipped with an energy dispersive X-ray spectroscope (EDS, Oxford INCA). X-ray powder diffraction (XRD) patterns (Cu $K\alpha$, λ=0.154 18 nm) were collected on a XPERTMPD θ-2θ diffractometer. The measured molar ratio of $n_K:n_{Gd}:n_{Mo}$ by microprobe elemental analysis is 6.95:7.04:15.07, which is in good agreement with the one determined from single crystal X-ray structure analysis.

After crystal structure determination, polycrystalline samples of $KGd(MoO_4)_2$ was synthesized by solid-state reactions of stoichiometric amounts ($n_K:n_{Gd}:n_{Mo}$=1:1:2) of analytical reagents of Gd_2O_3, K_2CO_3 and MoO_3. The pulverous mixtures were allowed to react at 1 023 K for 120 h. with several intermediate grindings in an opening Pt crucible.

1.2 Crystal structure determination and spectral measurement

A Prism-shaped single crystal of $KGd(MoO_4)_2$ with dimension of 0.10 mm×0.03 mm×0.02 mm was selected for single-crystal X-ray diffraction determination. The diffraction data were collected on a Rigaku Mercury CCD diffractometer with graphite-monochromated Mo $K\alpha$ radiation(λ=0.071 073 nm) using the ω scan mode at 293 K. Lorentz and polarization corrections were applied to all data, and an empirical absorption correction was applied using Crystal Clear[12] program. The crystal structures for the title complexes were solved by the charge-flipping method using the Superflip program and subsequently refined by the JANA2006 crystallographic computing system[13]. All non-hydrogen atoms in the structure were refined using harmonic anisotropic atomic displacement parameters (ADP). Crystal data, collected reflections and parameters of the final refinement are summarized in Table 1. Selected bond lengths and angles are

given in Table 2 and 3, respectively.

CSD: 427391.

The samples used for spectral measurements are polycrystalline powder synthesized by solid-state

Table 1　Crystal data and structure refinements for $KGd(MoO_4)_2$

Formula	$KGd(MoO_4)_2$	Absorption correction	Multi-scan
Software	JANA2006	Absorption coeffient / mm^{-1}	13.612
Formula weigh	516.23	$F(000)$	462
Wavelength / nm	0.710 73	Crystal size / mm	0.100×0.030×0.020
Crystal system	Triclinic	θ range / (°)	3.23~27.48
Space group	$P\bar{1}$	Limiting indices	(−6, −7, −13) to (6, 8, 13)
a / nm	0.529 23(6)	R_{int}	0.019
b / nm	0.692 10(6)	Reflections collected	1 543
c / nm	1.068 89(7)	Independent reflections	1 307
α / (°)	75.79(8)	Parameter / restraints / constraints	110 / 0 / 0
β / (°)	76.79(5)	GOF (gt)	1.36
γ / (°)	67.60(4)	Final R indices (gt)	R_1=0.022 8, R_2=0.028 2
Volume / nm^3	0.346 89(5)	R indices (all data)	R_1=0.026 4, R_2=0.029 3
Z	2	Largest difference peak and hole	0.60 and −0.48
D_c / ($g\cdot cm^{-3}$)	4.940 6		

Table 2　Atomic coordinates and equivalent isotropic displacement parameters for compound $KGd(MoO_4)_2$

Atom	Site	S.O.F	x	y	z	U_{eq}[a]
K1	2i	1	0.114 48(19)	0.195 20(15)	0.056 85(9)	0.010 1(6)
Gd1	2i	1	0.122 05(4)	0.685 59(3)	0.560 85(2)	0.006 44(11)
Mo1	2i	1	0.615 62(7)	0.929 01(6)	0.329 09(3)	0.006 13(12)
Mo2	2i	1	0.364 62(8)	0.561 18(6)	0.215 74(4)	0.007 73(12)
O1	2i	1	0.540 4(6)	0.687 79	0.414 49	0.010 1(6)
O2	2i	1	0.116 3(6)	0.560 39	0.370 06	0.011 5(7)
O3	2i	1	0.253 0(6)	0.687 9(5)	0.414 4(3)	0.017 1(7)
O4	2i	1	0.404 5(6)	0.560 2(5)	0.370 0(3)	0.018 7(7)
O5	2i	1	0.822 8(6)	0.500 5(5)	0.097 0(3)	0.014 0(7)
O6	2i	1	0.301 1(6)	0.804 7(5)	0.153 6(3)	0.011 7(7)
O7	2i	1	0.802 6(6)	0.913 8(5)	0.180 5(3)	0.011 3(7)
O8	2i	1	0.303 7(6)	0.624 8(5)	0.751 9(3)	0.012 8(7)

[a] U_{eq} is defined as one third of the trace of the orthogonalized U_{ij} tensor.

Table 3　Selected bond lengths (nm) and angles (°) for $KGd(MoO_4)_2$

Gd1-O6	0.232 5(3)	Mo1-O5	0.171 2(3)	K1-O4^{xi}	0.263 1(4)
Gd1-O2^{i}	0.237 1(3)	Mo1-O8	0.172 7(3)	K1-O5^{ix}	0.273 5(3)
Gd1-O1	0.240 5(3)	Mo1-O7	0.179 8(3)	K1-O3^{viii}	0.275 0(4)
Gd1-O2	0.241 5(3)	Mo1-O1	0.171 2(3)	K1-O6^{i}	0.277 0(4)
Gd1-O8^{ii}	0.241 7(3)	Mo2-O3	0.172 7(3)	K1-O5^{xii}	0.283 1(4)
Gd1-O7^{iii}	0.245 8(4)	Mo2-O4	0.179 8(3)	K1-O8^{xi}	0.295 0(3)
Gd1-O7^{iv}	0.248 6(3)	Mo2-O6^{v}	0.171 2(3)	K1-O4^{ix}	0.298 7(4)
Gd1-O1^{v}	0.251 1(3)	Mo2-O2	0.185 9(3)	K1-O3^{xi}	0.263 7(4)
O5-Mo1-O8	107.92(16)	O8-Mo1-O1	109.52(14)	O4-Mo2-O6^{v}	106.70(15)
O5-Mo1-O7	105.57(14)	O7-Mo1-O1	107.01(14)	O3-Mo2-O2	110.42(14)

Continued Table 3

O8-Mo1-O7	110.45(14)	O3-Mo2-O4	106.32(17)	O4-Mo2-O2	113.22(16)
O5-Mo1-O1	116.26(15)	O3-Mo2-O6^{v}	111.56(15)	O6v-Mo2-O2	108.59(15)

Note: ^{i} $-x$, $1-y$, $1-z$; ^{ii} $-x$, $2-y$, $1-z$; ^{iii} $-1+x$, y, z; ^{iv} $1-x$, $2-y$, $1-z$; ^{v} $1-x$, $1-y$, $1-z$; ^{viii} $-x$, $1-y$, $-z$; ^{ix} $1-x$, $1-y$, $-z$; ^{xi} x, $-1+y$, z; ^{xii} $-1+x$, $-1+y$, z.

reactions. To give evidence that the samples are of pure phase, we determined the powder XRD pattern using RIGAKU DMAX2500 diffractometer with Cu $K\alpha$ radiation (λ=0.154 18 nm) (step size of 0.05° and range 2θ=5°~65°). The powder XRD pattern is compared with the simulated ones, confirm the monophasic nature of the prepared sample (Fig.1). The absorption spectrum was recorded on a Lambda-35 UV/Vis spectrophotometer in the wavelength range of 200 ~ 800 nm. The emission spectrum was measured on a Cray Eclipse fluorescence spectrometer using Xe lamp at room temperature.

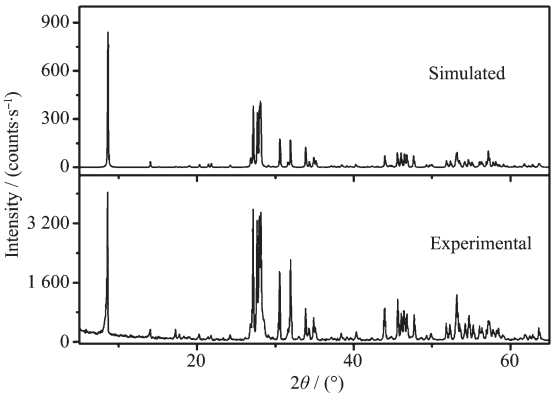

Fig.1 Experimental and simulated X-ray powder diffraction patterns of $KGd(MoO_4)_2$

1.3 Computational descriptions

The crystallographic data of $KGd(MoO_4)_2$ determined by X-ray is used for the theoretical calculations. Band structure calculations along with density of states (DOS) are performed with density functional theory (DFT) using one of the non-local gradient-corrected exchange-correlation functionals (GGA-PBE) and performed with the CASTEP code[14], which uses a plane wave basis set for the valence electrons and norm-conserving pseudopotential for the core electrons[15]. The number of plane waves included in the basis is determined by a cutoff energy of 450 eV and the numerical integration of the Brillouin zone is performed using a 4×3×2 Monkhorst-Pack k-point sampling. The interactions between the ionic cores and the electrons are described by the norm-conserving pseudopotential, in which the orbital electrons of K-$3s^23p^64s^1$, Gd-$4f^75s^25p^65d^16s^2$, Mo-$4d^55s^1$ and O-$2s^22p^4$ are treated as valence electrons.

The calculations of linear optical properties are also made in this work. The linear response of a system to an external electromagnetic field with a small wave vector is measured through the complex dielectric function $\varepsilon(\omega)=\varepsilon_1(\omega)+i\varepsilon_2(\omega)$. The imaginary part of the dielectric function, $\varepsilon_2(\omega)$, is given by the following equation:

$$\varepsilon_2(q\rightarrow O_{\hat{u}}, \hbar\omega)=\frac{2e^2\pi}{\Omega\varepsilon_0}\sum_{k,v,c}|<\Psi_k^c|\hat{u}\cdot r|\Psi_k^v>|^2\delta(E_k^c-E_k^v-E)$$

where c and v are band indexes, Ω is the volume of the system, and is the vector defining the polarization of the incident electric field. The imaginary part of the dielectric function, $\varepsilon_2(\omega)$, can be thought of as detailing the real transitions between the occupied and unoccupied electronic states. Since the dielectric constant describes a causal response, the real and imaginary parts are linked by a Kramers-Kronig transform[16].

$$\varepsilon_1(\omega)-1=\frac{2}{\pi}P\int_0^\infty\frac{\omega'\varepsilon^2(\omega')d\omega'}{\omega'^2-\omega^2}$$

and

$$\varepsilon_2(\omega)-1=\frac{2\omega}{\pi}P\int_0^\infty\frac{\varepsilon_1(\omega')d\omega'}{\omega'^2-\omega^2} \quad (2)$$

Here, the P means the principal value of the integral. This transform is used to obtain the real part of the dielectric function, $\varepsilon_1(\omega)$.

3 Results and discussion

3.1 Synthesis and crystal structure

The synthesis can be expressed by the following reaction:

$$K_2CO_3+Gd_2O_3+4MoO_3\rightarrow 2KGd(MoO_4)_2+CO_2$$

The X-ray diffraction analyses show that comp-

ound $KGd(MoO_4)_2$ belongs to α-$KEu(MoO_4)_2$-type structure family (space group $P\bar{1}$) as reported by Klevtsova et al[7]. The structure features a three-dimensional framework with MoO_4 tetrahedra, GdO_8 polyhedra and KO_8 polyhedra linked by corner-sharing O atoms, as shown in Fig.2. K and Gd atoms in this structure occupy their respective sites, while in potassium lanthanide molybdates $KLn(MoO_4)_2$ (Ln=Nd, Sm)[10], K and Ln atoms occupy the same crystallographic distinct site in ordering manner which induces the structure modulation. There is one unique potassium (I) atom, one gadolinium(Ⅲ) atom, two molybdenum(Ⅵ) atom, and eight oxygen atoms in the asymmetric unit of $KGd(MoO_4)_2$(Fig.3). The molybdenum(Ⅵ) atom is four coordinated by four oxygen atoms, forming isolated $[MoO_4]^{2-}$ anions. The $[MoO_4]^{2-}$ has a tetragonal structure, in which the Mo^{6+} is located at the center of the tetragonal structure with four O^{2-} located at the four apex angles. The Mo-O distances fall in the range of 0.171 2(3)~0.185 9(3) nm, and O-Mo-O bond angles range from 106.32(17) to 116.26(15)°, which are comparable to those reported in other metal molybdates[3-10]. Results of bond valence calculations indicate that the molybdenum atom is in +6 oxidation state[17]. The gadolinium atom is coordinated by eight oxygen atoms from eight $[MoO_4]^{2-}$ anions in a distorted square anti-prismatic geometry via corner-sharing O atoms. The Gd-O distances are in the range of 0.232 5(3)~0.251 1(3) nm. Each potassium atom is surrounded by eight oxygen atoms with K-O distances ranging from 0.263 1(4) to 0.298 7(4) nm. It is worth noting that here are four Gd-O weak contacts (0.375~0.392 nm) and two K-O contacts (0.387 7(3) and 0.392 7(4) nm), which can be considered as secondary coordination bonds to complete the extended coordination spheres of these large cations (coordination number up to 12 and 10 for Gd^{3+} and K^+, respectively). Isolated $[MoO_4]^{2-}$ anions adopt a linear array along *a*-axis, forming four directions one-dimensional (1D) Mo … Mo chains with the separations of about 0.525 nm. They are further interconnected by the Gd^{3+} cations into a 2D $[Gd(MoO_4)_2]^-$ anionic layer in the *ab*-plane. Alternatively, $[Gd(MoO_4)_2]^-$ anionic network can be described as interlocked GaO_8 polyhedra and MoO_4 tetrahedra, as shown in Fig.4. The $[Gd(MoO_4)_2]^-$ layers delimit infinite tunnels along the b-axis where K^+ cations are located, leading to a complicated 3D network of $KGd(MoO_4)_2$ (Fig.2).

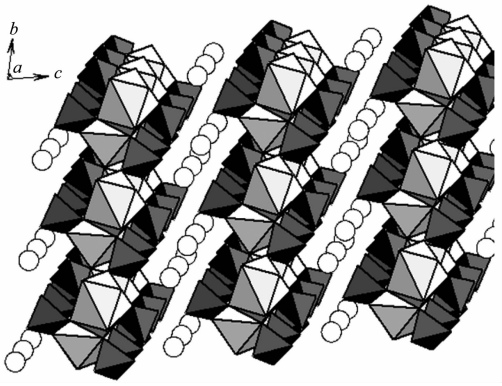

Fig.2　View of the crystal structure of $KGd(MoO_4)_2$ composed of MoO_4 tetrahedra(dark gray), GdO_8 polyhedra(light gray) and K atoms(white circles)

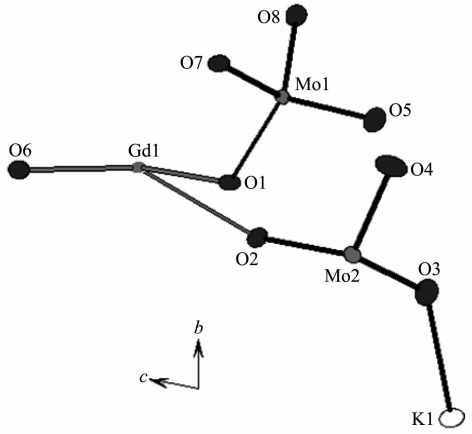

Fig.3　Asymmetric unit of $KGd(MoO_4)_2$

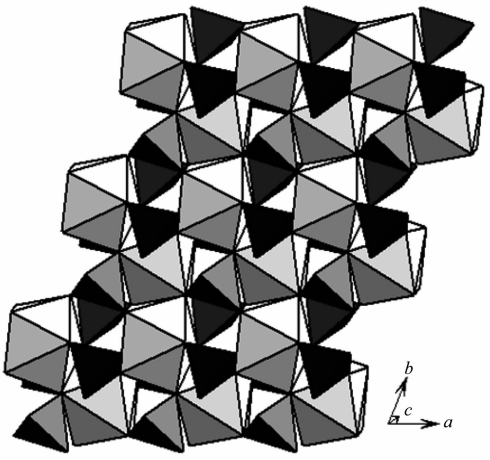

Fig.4　2D $[Gd(MoO_4)_2]^-$ anionic layer composed of MoO_4 tetrahedra and GdO_8 octahedra in the *ab*-plane

3.2 Fluorescence properties

Previous studies on complex $KGd(MoO_4)_2$ were usually focused on using it as host material for doping other rare-earth elements to generate fluorescence effect, including $KGd(MoO_4)_2$:Er^{3+}/Yb^{3+} [18a], $KGd(MoO_4)_2$:Eu^{3+} [18b], etc. However, to the best of our knowledge the emission spectra of itself have not been reported so far. The following section will discuss the emission spectra of KGd $(MoO_4)_2$ and the assignments of the electronic spectra in view of the band structure and density of states.

When the ultraviolet light of 265 nm is used to excite powder sample $KGd(MoO_4)_2$, emission bands ranging from 350 to 400 nm are observed, as shown in Fig.5. It is noted that the emitted energy is less than the optical absorption edge. The emission bonds ranging from 350 to 430nm are ascribed to the radiative transition within tetrahedral $[MoO_4]^{2-}$ group, where the exciton becomes autolocalised. When it is excited, one *p*-electron of O^{2-} ($2s^22p^6$) transfers to 5*d* empty shells of Mo^{6+}($5s^25p^6$) to form Mo^{5+} ($5s^25p^6d$), then transfers back to the ground state and generates transition radiation. Very strong and sharp optical emissions resulting from 4*f*-4*f* transitions of lanthanide atom are not observed at the ultraviolet region. The close distance of Gd-Gd, which is about 0.39 nm according to crystal structure determination, possibly results in the fluorescence quenching due to the interaction among Gd^{3+} ions. In addition, emission band at around 422 nm is observed, which possibly results from 5*d*-4*f* electronic transitions of the Gd^{3+} ion or from defects.

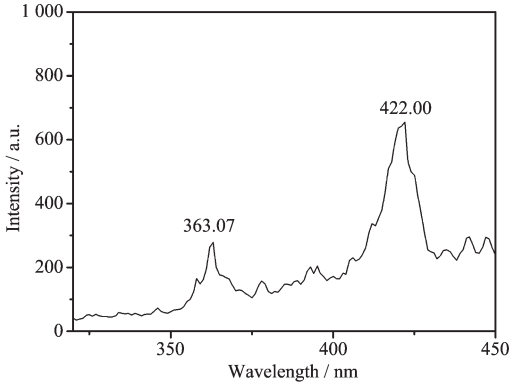

Fig.5 Emission spectra of $KGd(MoO_4)_2$ (excited at 265 nm)

3.3 Theoretical studies

Here, we calculate the energy band structures, density of states (DOS), and the linear optical response properties of crystal $KGd(MoO_4)_2$ by the DFT method. The spin polarization is properly taken into account because of the unpaired f-electron effect of the Gd^{3+} ion. The calculated band structure along high symmetry points of the first Brillouin zone is plotted in Fig.6, where the labeled k-points are present as G (0.0, 0.0, 0.0), F (0.0, 0.5, 0.0), Q (0.0, 0.5, 0.5) and Z (0.0, 0.0, 0.5). Both the top of valence bands (VBs) and the bottom of conduction bands (CBs) display a small dispersion. The state energies (eV) of the lowest conduction band (L-CB) and the highest valence band (H-VB) at some *k*-points of the crystal $KGd(MoO_4)_2$ are listed in Table 4. The lowest energy (3.20 eV) of conduction bands (CBs) is localized at the G point whereas the highest energy (0.00 eV) of valence bands (VBs) is localized at the Z point. Hence, $KGd(MoO_4)_2$ is an indirect band-gap semiconductor.

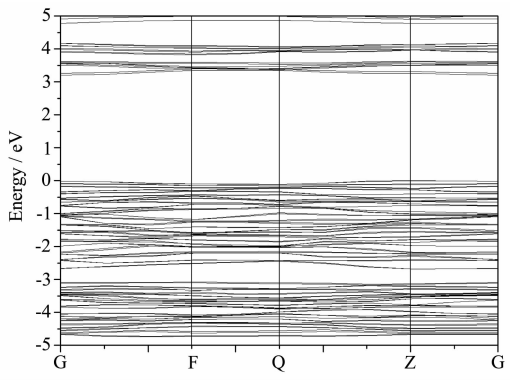

Fig.6 Calculated energy band structure of $KGd(MoO_4)_2$ in the range from −5.0 to 5.0 eV; Fermi level is set at 0.0 eV

On the other hand, the experimental optical diffuse reflectance absorption spectrum of the title compound is shown in Fig.7. The absorption edge is around 375 nm (3.31 eV) which might be considered as the band gaps of the corresponding compound. Accordingly, the calculated indirect band gap of 3.20 eV is smaller than the corresponding experimental value of 3.31 eV. The little discrepancy is due to the limitation of DFT method that generally

Table 4　State energies (eV) of the lowest conduction band (L-CB) and the highest valence band (H-VB) at some *k*-points of the crystal $KGd(MoO_4)_2$

k-point	G	F	Q	Z
L-CB	3.202	3.355	3.353	3.258
H-VB	−0.016	−0.095	−0.104	0.000

underestimates the band gap in semiconductors and insulators. For the unconspicuous difference of band gap value, no scissor operator is applied for the calculations of DOS for the title compound.

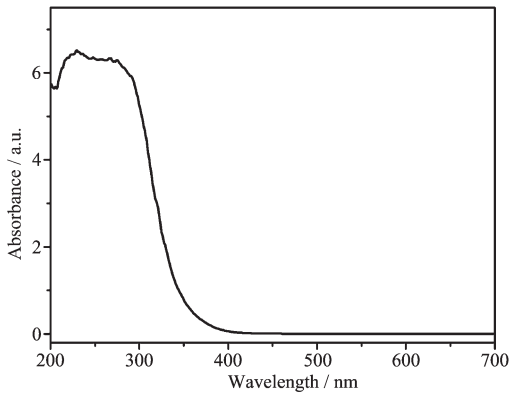

Fig.7　Absorption spectra of $KGd(MoO_4)_2$

The total and partial densities of states (DOS) are plotted in Fig.8. The regions below the Fermi level (the Fermi level is set at the top of the valence band) contain 94 bands (two formula units/unit cell) and can be divided into five regions. The states of Gd-5*s* form the VBs lying near −40.0 eV, and the states of K-3*s* lying near −26.4 eV. The VBs ranging from −21.5 to −14.5 eV are composed of the states of Gd-5*p*, Mo-5*s* and O-2*s* states. The VBs near −10.5 eV are dominated by K-3*p* with small mixings of Mo-4*d* states. The fifth region of the VBs between −6.20 eV and the Fermi level (0.0 eV) is dominated by the O-2*p*, mixing with small amount of K-3*s*3*p*, Gd-5*s*5*p*5*d*, Mo-5*s*, Gd-4*f* and Mo-4*d* states. The CBs in the range of 3.0 eV and 4.5 eV are mostly contributions from Mo-5*s*.

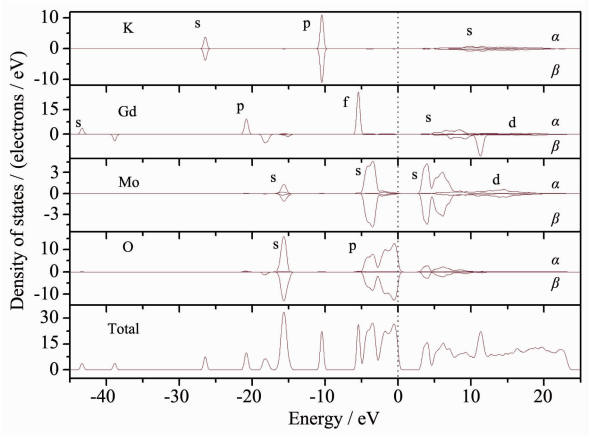

Fig.8　Total and partial DOS of $KGd(MoO_4)_2$

Experimental study shows that the absorption edge of $KGd(MoO_4)_2$ is at about 400 nm, and the strong absorption peak is at around 250 nm, while there is no absorption above 400 nm. To evaluate and assign the observed absorption spectra, we examined the linear optical response properties of it. The imaginary part $\varepsilon_2(\omega)$ and the real part $\varepsilon_1(\omega)$ of the frequency-dependent dielectric function were calculated without the DFT scissor operator approximation. It is found from the dispersion of the calculated $\varepsilon_2(\omega)$ spectra from 200 to 650 nm (Fig.9) that the maximum absorption peaks are located at about 270 nm, and there is no absorption above 400 nm. It is comparable to the experimental data as mentioned above; hence, our calculated value is reasonable. According to the above DOS analysis, the absorption ranging from 200 to 300 nm is mainly attributed to the charge transfers from O-2*p* to Mo-5*s* states.

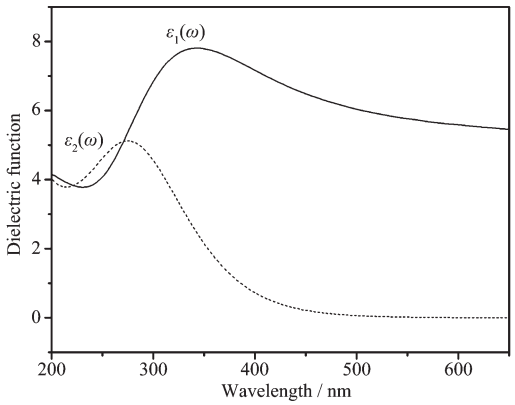

Fig.9　Calculated real and imaginary parts of dielectric functions of $KGd(MoO_4)_2$ in polycrystalline calculation geometry

Acknowledgment: This work was supported by National

Science Foundation of China (Grant No. 21201056) and Technology Office of Henan(No. 122300410418).

References:

[1] (a)Nesterenko N M. *Phys. Solid. State*, **2000**,**42**:184-188
(b)Kharchenko N F, Kharchenko Yu N. *Low. Temp. Phys.*, **1998**,**24**:689-699
(c)Morozov V A, Arakcheeva A V, Chapuis G, et al. *Chem. Mater.*, **2006**,**18**:4075-4082
(d)Pashchenko V A, Jansen A G M, Kobets M I, et al. *Phys. Rev. B*, **2000**,**62**:1197-1202
(e)Mczka M, Kojima S, Hanuza J. *J. Phys. Soc. Jpn.*, **1999**, **68**:1948-1953
(f)Galceran M, Pujol M C, Aguilo M. *J. Sol-gel. Sci. Technol.*, **2007**,**42**:79-88
(g)Silvestrea O, Pujola M C, Soléa R, et al. *Mat. Sci. Eng. B-Solid*, **2008**,**146**:59-64

[2] (a)Sillen L G, Nylander A L. *Arkiv. Foer. Kemi, Mineralogi. Och. Geologi.*, **1943**,**17**:27-33
(b)Dickinson R G. *J. Am. Chem. Soc.*, **1920**,**42**:85-93

[3] Klevtsova R F. *Crystallogr. Rep.*(*Kristallografiya*), **1975**,**20**: 746-750

[4] Egorova A N, Maier A A, Nevskii N N, et al. *Izve. Akad. Nauk. SSSR, Neorg. Mater.*, **1982**,**18**:2036-2038

[5] Klevtsova R F, Klevtsov P V. *Crystallogr. Rep.*(*Kristallografiya*), **1970**,**15**:466-470

[6] Klevtsova R F, Vinokurov V A, Klevtsov P V. *Crystallogr. Rep.*(*Kristallografiya*), **1972**,**17**:284-288

[7] Klevtsova R F, Kozeeva L P, Klevtsov P V. *Crystallogr. Rep.* (*Kristallografiya*), **1974**,**19**:89-94

[8] Klevtsova R F, Borisov S V. *Dokl. Akad. Nauk. SSSR*, **1967**, **177**:1333-1336

[9] Chaninova S D, Kuznetsov V P, Lakin E E, et al. *Ferroelectrics*, **1996**,**175**:85-89

[10](a)Arakcheeva A, Chapuis G. *Acta Cryst.*, **2008**,**B64**:12-25
(b)Morozov V A, Arakcheeva A V, Chapuis G, et al. *Chem. Mater.*, **2006**,**18**:4075-4082
(c)Arakcheeva A, Pattison P, Chapuis G, et al. *Acta Cryst.*, **2008**,**B64**:160-171

[11](a)Lazoryak B. *X-ray Powder Diffraction Laboratory of Chemistry Technology*, Moscow State University, Russia, ICDD Grant-in-Aid, **2001**.
(b)Wanklyn B M, Wondre F R. *J. Cryst. Growth.*, **1978**,**43**: 93-100
(c)Savel′eva M V, Shakno I V, Plyushchev V E, et al. *Russ. J. Inorg. Chem.*, **1970**,**15**:425-429

[12](a)Rigaku. *Crystal Clear*. Rigaku Corporation, Tokyo, Japan., **2004**.
(b)Higashi, T. *ABSCOR*. Rigaku Corporation, Tokyo, Japan, **1995**.

[13](a)Palatinus L, Chapuis G. *J. Appl. Crystallogr.*, **2007**,**40**: 786-790
(b)Petříček V, Dušek M, Palatinus L. Jana 2006, *The Crystallographic Computing System*, Institute of Physics, Praha, Czech Republic, **2006**.

[14](a)Segall M, Linda P, Probert M, et al. *Materials Studio CASTEP*, Version 2.2; San Diego, CA: Accelrys, Inc., **2002**.
(b)Segall M, Linda P, Probert M, et al. *J. Phys.*: *Condens. Matter.*, **2002**,**14**:2717-2744

[15]Hamann D R, Schluter M, Chiang C. *Phys. Rev. Lett.*, **1979**, **43**:1494-1497

[16]Macdonald J R, Brachman M K. *Rev. Mod. Phys.*, **1956**, **104**:393-422

[17]Brown I D. *J. Appl. Cryst.*, **1996**,**29**:479-480

[18](a)Chen Q J, Qin L J, Feng Z Q, et al. *J. Rare Earths*, **2011**, **29**(9):843-848
(b)Yi L H, Zhou L Y, Wang Z L, et al. *Curr. Appl. Phys.*, **2010**,**10**(1):208-213